

Characterization of Monocrystalline β -SiC Thin Film Grown by Chemical Vapor Deposition

H. J. Kim¹ and R. F. Davis²

¹Dept. of Inorganic Materials Engineering

Seoul National University, Seoul, Korea

²Dept. of Materials Science and Engineering

North Carolina State University, Raleigh, NC, USA

ABSTRACT

High quality monocrystalline β -SiC thin films were grown via two-step process of conversion of the Si(100) surface by reaction with C_2H_4 and the subsequent chemical vapor deposition (CVD) at 1360°C and 1 atm total pressure. Four dopants, B and Al and p-type, and N and P for n-type, were also incorporated into monocrystalline β -SiC thin films during the CVD growth process. IR and Raman spectroscopies were used to evaluate the quality of the undoped β -SiC thin films and to investigate the effects of dopants on the structure of the doped β -SiC thin films. The changes in the shape of IR and Raman spectra of the doped thin films due to dopants were observed. But the XTEM micrographs except for the B-doped and annealed films showed the same density and distribution of stacking faults and dislocations as was seen in the undoped samples. The IR and Raman spectra of the B-doped and annealed films showed the broad and weak bands and one extra peak at the 850 cm^{-1} respectively. The SAD pattern and XTEM micrograph of the B-doped and annealed film provided the evidence for twinning.

I. INTRODUCTION

Cubic β -silicon carbide (zinc-blende structure) attracts great interest as a promising semiconductor material for high temperature, high power, or high-speed devices because of its special physical and electronic properties^{1,2}. In addition, monocrystalline β -SiC possesses the transparency to visible light and thus it is also regarded as a candidate material for optoelectronic devices.

A limited number of studies have been conducted to characterize β -SiC using optical analysis techniques such as IR absorption and Raman scattering since it was very difficult to grow the relatively pure and sizable monocrystalline β -SiC thin films of around 10 mm diameter and around 10 μm thickness were successfully and reproducibly grown on Si (100) substrates via CVD technique³.

Optical characterization is an important and useful method to illustrate the lattice vibrating modes and atomic arrangement in crystals. IR absorption spectrum of β -SiC was reported by Spitzer et al.⁴ and Akimchenko et al.⁵ The shape of spectrum was very similar to that of α -SiC, such as 15R- and 6H-SiC, observed by Spitzer et al.⁶, Lipson⁷ and Patrick and Choyke.⁸ The reason for these similarities may be because the characteristic phonon frequencies of different polytypes of SiC are similar.

The Raman spectrum is a measure of the density of vibrational states and illustrates the short-range order of the crystals. β -SiC has a zinc-blende structure and is partially ionic. Therefore, a separation of the TO and LO modes at the Brillouin zone (BZ) center ($k = 0$) takes place. Phonons from these branches near the center of the BZ are Raman active.¹⁰ Two characteristic phonon peaks of β -SiC firstly reported by Feldman et al.¹¹ take place at 796 and 972 cm^{-1} for TO and LO, respectively.

The effects of ion bombardment induced damage on the crystalline structure of β -SiC were reported by Wright and Gruen.¹² The ion damage can alter the pure-crystal space group selection rules allowing new phonon modes to be observed or it can change the polarization properties of allowed phonon modes. Even when the ion damage is not great enough to alter the symmetry based selection rules, the effect of the damage can manifest itself by broadening the allowed phonon peaks and by shifting the observed phonon frequencies. These effects may be the result of stresses and strains arising as the incident ion dissipates its energy in the ion bombardment process. The pressure dependence of Raman phonon modes of β -SiC was reported by Olego and Cardona.¹³ They found that the positions of LO and TO were moved to higher Raman shift and the LO-TO splitting of β -SiC increased with increasing pressure up to 22.5 GPa. The effect of dopants on the Raman spectrum of β -SiC has not been studied but Raman scattering experiments of other semiconductors such as 6H-SiC,¹⁴ Si,^{15,16} GaP,^{17,18} and CdMnTe¹⁹ were conducted. Raman phonon frequency generally decrease with increasing doping concentration in semiconductors. This results can be interpreted in terms of the calculated self energy for phonons interacting with free electrons.

II. EXPERIMENTAL PROCEDURES

The β -SiC films with (100) surfaces and with thickness in the range from 10 to 30 μm were used for optical characterization. Prior to analyses, the silicon substrate of each sample was completely etched away using a 1:1 HF+HNO₃ mixture. The β -SiC films were transparent and had amber yellow color and a highly reflective top surface. In general, the spectra were obtained both on the as-grown and on the annealed sample, which were annealed at 2073 °K for 300 s in 1 atm Ar atmosphere. For the as-grown samples, no additional sample preparation was performed after removing the Si substrate.

The IR transmission measurements were made at room temperature by the conventional sample in-sample out technique, using a Perkin-Elmer double beam spectrometer. A beam condenser facilitated the analysis of very small samples. For IR reflection measurements, a specular reflectance accessory, which consisted of several reflecting mirrors, was employed. A typical sample size used for all these experiments as 0.003 \times 0.005 m. The sample was placed on a 0.002 m diameter hole of the sample holder using a small amount of sticky petroleum jelly. The measurements scanned the wavelength range from 5.6 to 25 μm (400-1800 cm^{-1}).

Raman spectra were taken at room temperature using the back-scattering geometry standard for transparent samples. All measurements were conducted with the 514.5 nm line of an argon ion laser operating at an approximate 0.5 KW power level. The laser beam was focused onto the sample with a cylindrical lens. A typical spectral slit width used was 0.001 m and thus the resolution was 10 wave numbers. The spectra were analyzed with a Spex double monochromator equipped with photon detection and counting electronics. Counting times from 1 to 10 seconds were used.

The development of sample preparation procedures for cross-sectional TEM (XTEM) has allowed two advantages. The first is that the Si substrate, the thin film, and the interfaces between them can be imaged either simultaneously or individually. The second advantage is that the XTEM technique can eliminate the problems of superposition that are a consequence of viewing a layered structure in the plan-view TEM. The disadvantage is that the total procedure for preparing XTEM specimens is difficult, time-consuming and very tedious. The β -SiC film on Si substrate was sectioned into two rectangular slabs, that measured at least 0.004 m in width and about 0.006 m in length using a low speed diamond saw. The two slabs were glued together to make a single sandwich structure with epoxy. Two dummy Si slabs were also glued on both sides of SiC/Si slabs to provide extra support. The sandwich structure was then clamped in a small squeezing vise and baked in vacuum at 383 °K for 3600 seconds

to cure the epoxy. Several slices, of which thickness was about 500 μm , were produced from the sandwich structure perpendicular to the planar surface. These slices were lapped to a thickness of 50-75 μm using SiC paper and polished on both sides to a 0.3 μm Al_2O_3 finish. Dimpling of the specimen was conducted using 1 μm diamond paste until the thickness of the sample at the center of the dimple was about 10 μm . After dimpling, the sample was mounted on a 3 mm OD \times 1.5 mm ID \times 25 μm thick Mo ring using a low vapor pressure epoxy. The final step in the preparation sequence was Ar ion milling of the sample to electron transparency. Argon ions accelerated in 5.5 KV potential were employed and a specimen tilt angle was normally between 5 and 10 degrees.

III. RESULTS AND DISCUSSION

A. IR Absorption Spectra

IR transmission spectrum of as-grown β -SiC thin film with a thickness of about 20 μm is shown in Figure 1. In the region between 400 and 700 cm^{-2} (19-25 μm), there are no bands except several interference fringes which appear due to the thickness of the β -SiC film. The reflective index in this region is not constant since the width of fringes decreases as the wave number increases. This phenomenon was observed in the theoretically calculated reflective index data reported by Spitzer et al.⁴ The deep and flat band appeared in the 740 to 1000 cm^{-1} (10-13.5 μm) region of the IR transmission spectrum corresponds to the very strong, broad Reststrahlen band in the reflection spectrum in Figure 2 and appears in the neighborhood of the optical lattice phonon modes, LO and TO. As a consequence of the infrared dispersion by the slight ionic characteristics of Si-C bonding, electromagnetic radiation, with frequencies in the vicinity of the dispersion frequency, undergoes selective reflection. This selective reflection of radiation in the neighborhood of the optical lattice mode frequencies, known as the Reststrahlen phenomenon, is common in ionic crystals¹⁰

Several bands are observed in the 700 to 1800 cm^{-1} (5.5-10 μm) region, as shown in Figure 1. These bands can be interpreted as combinations of the four lattice phonon modes as in the same way as Patrick and Choyke⁸ did for 6H and 15R SiC. It is surprising that the shapes and the positions of the bands in Figure 1 and 2 are very similar to all the other polytypes reported by Spitzer et al.,⁶ Lipson,⁷ Patrick and Choyke⁸ and Akimchenco et al.⁵

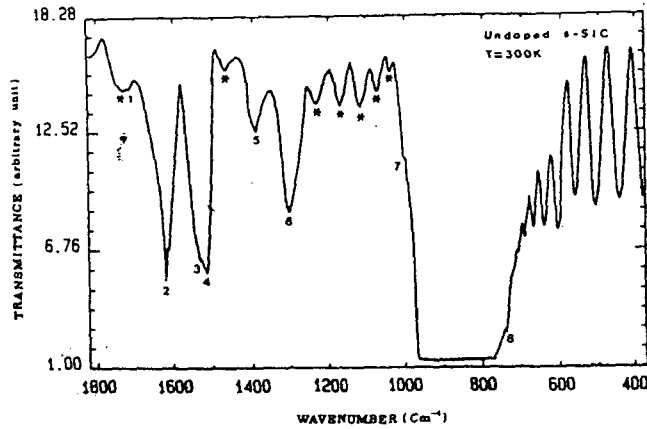


Figure 1. IR transmission spectrum of an as-grown and undoped β -SiC thin film which has been removed from the Si substrate.

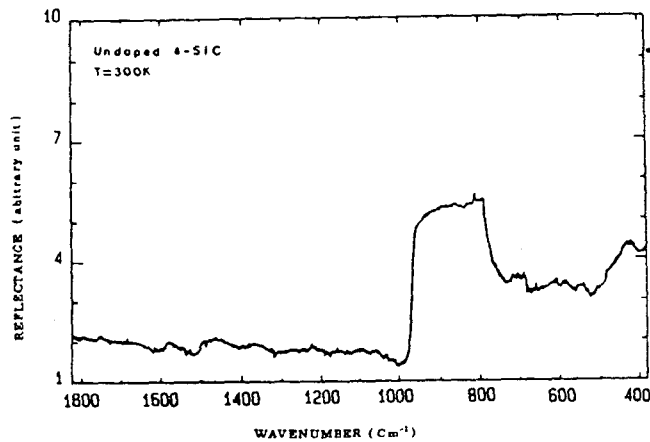


Figure 2. IR reflection spectrum of the as-grown undoped β -SiC film.

The reason for these similarities may be because the characteristic phonon frequencies of different polytypes of SiC^{20} are similar. These similarities prove Patrick's conclusion⁸ that a change from the cubic polytype to the more complicated structures of the 6H and 15R polytypes does not introduce any additional strong singularities into the phonon spectrum.

All singularities in the 700 to 1800 cm^{-1} are marked with numbers or asterisks (*). Since bands marked with asterisks disappear or change their positions as the thickness of SiC sample changes, these bands may be regarded as the interference fringes due to the thin thickness of SiC sample. However, the bands marked with numbers appear at the same wave number although the thickness of sample varies.

Patrick and Choyke⁸ used phonon frequencies, 363, 541, 771, and 851 cm^{-1} for TA, LA, TO and LO phonons, respectively, and successfully assigned the combinations of four phonon modes to IR transmission bands in the 700 to 1800 cm^{-1} region of 6H and 15R SiC polytypes. Although they fit the combination bands, the frequency of LA phonon mode, 541 cm^{-1} is far from the 'interband' LA phonon frequency, 641 cm^{-1} , which was obtained by Choyke et al.²⁰ using photoluminescence technique. In addition, they also failed to find any bands or singularities for 2TA and 2LA combination modes. However, we can assign combination mode to each band differently from Patrick and Choyke's work⁸ by designating 2LO, 2TO, 2LA and 2TA to bands numbered 1, 3, 6 and 8, respectively. Under this assumption the frequencies of TA, LA, TO and LO phonon modes are selected to be 373, 654, 768 and 855 cm^{-1} , respectively. The combination bands, TO+TA, and LO+TA don't appear in the frequencies of 1141 and 1228 cm^{-1} , respectively. The reason for this may be because strong interference fringes interrupt the appearance of these phonon modes. Although some of bands are slightly misfitted with the assigned frequencies, all bands of IR transmission spectrum are able to interpreted as two-phonon combination modes and the assigned and observed frequencies of bands in IR transmission spectrum are shown in Table 1.

Table 1. Observed and assigned combination band frequencies

Combination Bands	Observed Frequencies (cm^{-1})	Assigned Frequencies (cm^{-1})	Marked Number
2LO	1710	1710	1
TO+LO	1622	1623	2
2TO	1536	1536	3
LO+LA	1518	1509	4
TO+LA	1400	1422	5
2LA	1308	1308	6
TO+TA	-	1141	-
LO+TA	-	1228	-
LA+TA	1010	1027	7
2TA	746	746	8

Figure 3 shows the IR transmission and reflection spectra in the 400-1800 cm^{-1} range for as-grown Al-doped (atomic concentration of $1.0 \times 10^{19} \text{ cm}^{-3}$) β -SiC film. The shapes

of both spectra are almost the same as those of the undoped β -SiC film shown in Figure 1 and 2.

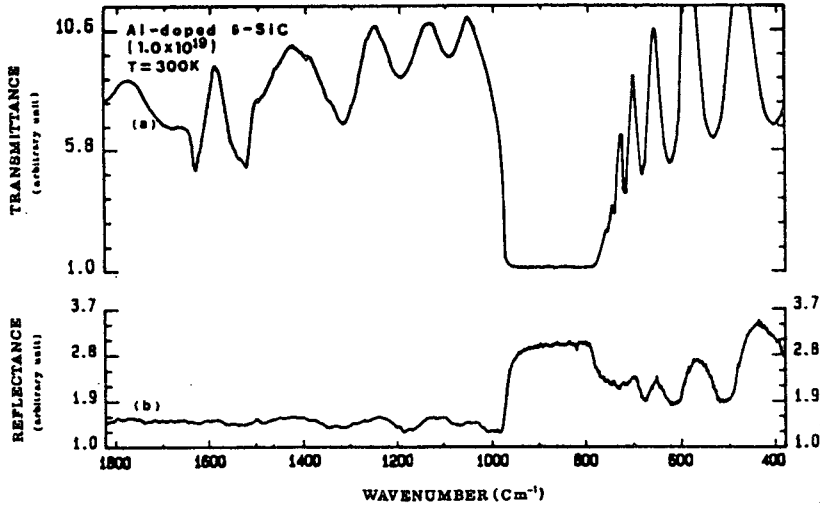


Figure 3. Room temperature IR spectra for Al-doped ($1.0 \times 10^{19} \text{ cm}^{-3}$) β -SiC in the range of 400 to 1800 cm^{-1} ; (a) absorption in an as-grown sample, (b) reflection from an as-grown sample.

However, in this doped sample, the intensity of the transmission of the combination TO+TA band decreases, although that of the 2LO peak increases relative to those in the transmission spectrum of undoped β -SiC. The shape of the IR spectra of the Al-doped sample annealed at $2073 \text{ }^\circ\text{K}$ for 300 s is the same as that of the as-grown Al-doped sample, and thus is not shown. This result implies that the heavily added Al atoms don't affect the Si-C vibrating mode considerably and that the ionization ratio of Al dopants is too low. It was reported that the ionization ratio was about 0.001 for Al dopant.²¹

The as-grown and heavily N-doped (atomic concentration of $7.4 \times 10^{19} \text{ cm}^{-3}$) β -SiC film has the same order of dopant concentration as the Al-doped sample but the absorption and reflection spectra of N-doped sample are much different showing no strong absorption and reflection bands, as shown in Figure 4.

The unannealed N-doped β -SiC absorbs the entire IR light in this frequency range (400 - 1800 cm^{-1}). Low transmittance and no strong bands imply that N dopants change the microstructure of SiC crystals and thus the lattice vibration modes in β -SiC crystals. After annealing at $2073 \text{ }^\circ\text{K}$ for 300 s, the spectrum of N-doped β -SiC film inclines in the 1100 to 1800 cm^{-1}

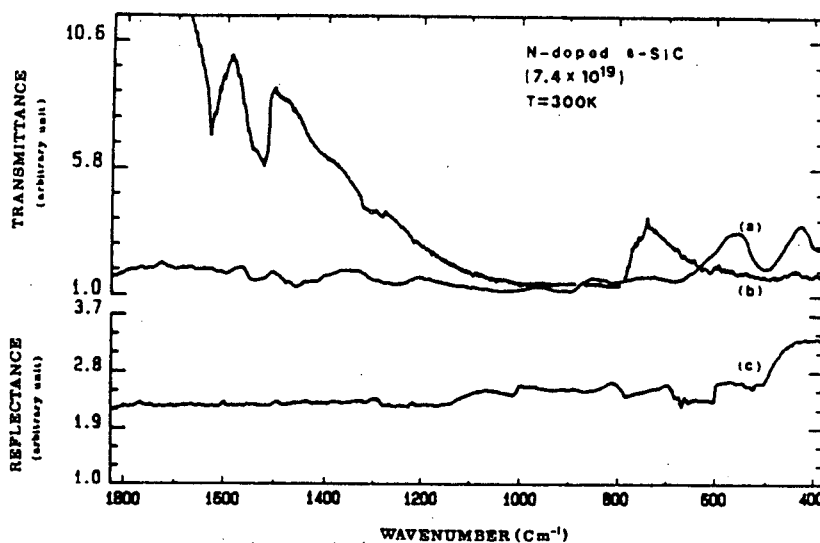


Figure 4. Room temperature IR spectra for N-doped ($7.4 \times 10^{19} \text{ cm}^{-3}$) β -SiC in the range of 400 to 1800 cm^{-1} ; (a) absorption in an as-grown sample, (b) adsorption in the sample annealed at 2073 $^{\circ}\text{K}$ for 300 s, (c) reflection from an as-grown sample.

region and shows relatively weak lattice absorption bands. The same phenomenon was also observed in the light green SiC sample, which contained impurities, by Lipson.⁷ Thus the intentionally added N atoms result in the inclined tail and the weak lattice absorption bands. The change between the IR transmission spectrum of the as-grown N-doped and that of the annealed β -SiC films may be explained by two possible reasons. One is because the annealing process improves the microstructure of β -SiC crystal and thus increases a freedom of lattice vibration. Another is that during annealing process the N dopants escaped from the β -SiC sample and thereby the concentration of dopants was reduced since the annealing process was done at high temperature of 2030 $^{\circ}\text{K}$.

Except for the low absorption of the 2LO peak, the IR spectra of the as-grown P-doped (atomic concentration of $1.2 \times 10^{17} \text{ cm}^{-3}$) β -SiC shown in Figure 5 are identical to those of the undoped β -SiC.

This similarity is very likely due to the low doping concentration. The shape of the IR spectra of the P-doped samples annealed at 2073 $^{\circ}\text{K}$ for 300 s is the same as that of the unannealed sample, and thus is not shown. Since the heavily P-doped samples are translucent and partially polycrystallized, the IR spectra for the heavily P-doped samples have not been obtained. The unannealed and lightly B-doped (atomic concentration of $1.6 \times 10^{17} \text{ cm}^{-3}$) β -SiC

films show the identical IR spectra (both transmission and reflection) to those of the undoped β -SiC in the 400-1000 cm^{-1} range, as shown in Figure. 6.

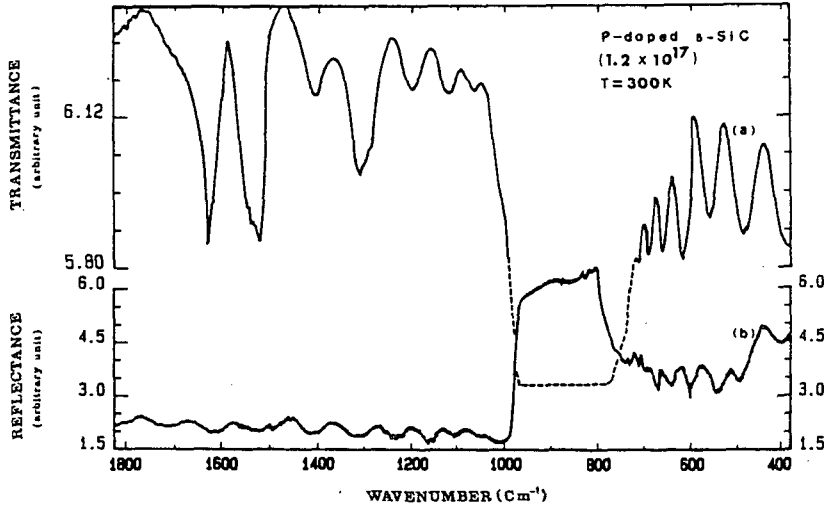


Figure 5. Room temperature IR spectra for P-doped ($1.2 \times 10^{17} \text{ cm}^{-3}$) β -SiC in the range of 400 to 1800 cm^{-1} ; (a) absorption in an as-grown sample, (b) reflection from an as-grown sample.

Room temperature IR spectra for B-doped ($1.6 \times 10^{17} \text{ cm}^{-3}$) β -SiC

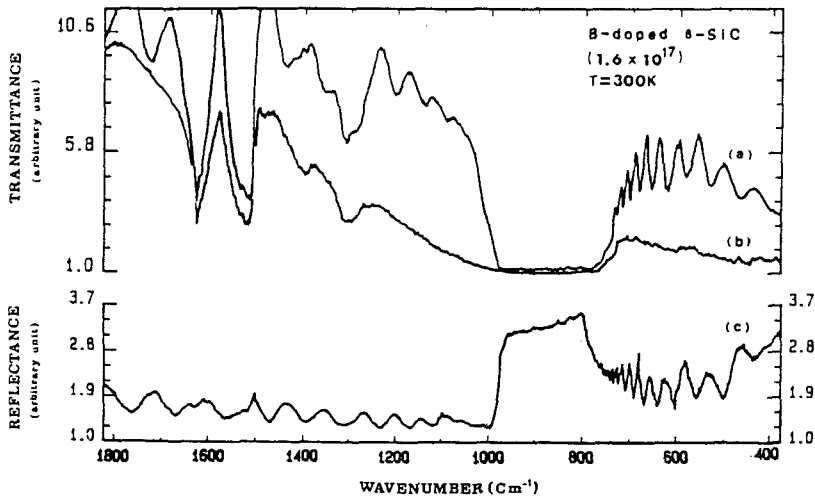


Figure 6. Room temperature IR spectra for B-doped ($1.6 \times 10^{17} \text{ cm}^{-3}$) β -SiC in the range of 400 to 1800 cm^{-1} ; (a) absorption in an as-grown sample, (b) absorption in the sample annealed at 2073 $^{\circ}\text{K}$ for 300 s, (c) reflection from an as-grown sample.

However, the transmission spectrum of the B-doped sample annealed at 2073 °K for 300 s shows weak absorption bands as well as a broad Reststrahlen band similar to that in the IR transmission spectrum of the annealed N-doped sample in Figure 3. The presence of this broad and weak bands indicates that the crystal structure of the annealed B-doped sample is more deformed than that of the unannealed sample. Although the result is different from those of other doped samples, it is consistent with the result of XTEM, which will be discussed in the last section. The IR spectra for the heavily B-doped sample were not taken because of its polycrystallinity.

B. Raman Spectra

Raman spectra of the 450 to 1100 cm^{-1} region for the undoped β -SiC films were obtained under the following conditions: a) as-grown, laser beam reflected from an interface between the Si and the SiC, b) as-grown, laser beam reflected from the surface of the SiC film, and

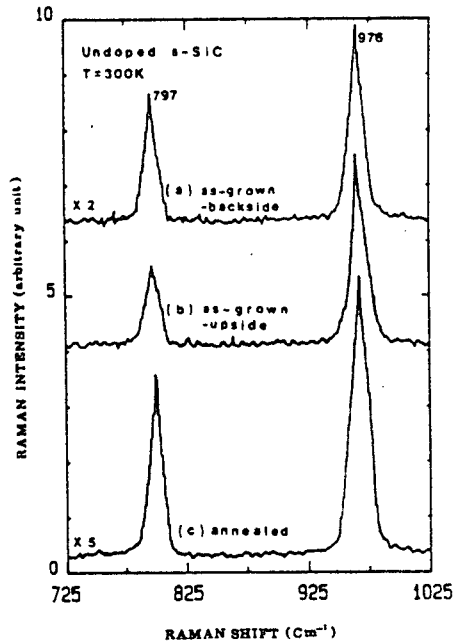


Figure 7. Raman spectra of an as-grown and undoped β -SiC film at 300 °K obtained without the presence of the Si substrate (a) from the backside (interference between Si and SiC), (b) from the upside of the as-grown sample, (c) from the annealed sample.

c) after annealing at 2070 °K for 300 s, laser beam reflected from the surface. Two prominent first order Raman peaks, TO and LO, at 797 and 975 cm^{-1} , respectively, agree within experimental error with the values reported by other authors.^{10,11,13}

The spectrum from the surface of the film has less intensity than that from the interface of the film, as can be seen in Figure 7.

This difference in intensity may be caused by the fact that the surface is generally rougher than the interface, and thereby enhances the diffuse reflection of the laser beam. After annealing at 2070 °K for 300 s, the intensities of the two phonon modes increases considerably.

This increased intensity indicates of the two phonon modes increase considerably. This increased intensity indicates that a better structural arrangement of the Si and C atoms in the crystal was accomplished after annealing. Those spectra of these undoped β -SiC films do not show the presence of "free" silicon or carbon that is indicated by the absence of bands at 520 cm^{-1} and 1580 cm^{-1} , respectively. In addition, no significant LO-TO splitting and no second-order Raman bands due to residual stress in the SiC film were observed in this study. The intensity ratio of LO to TO is about 1.5.

Figure 8 shows the unpolarized Raman spectra obtained at 300 °K for the Al doped SiC sample having an atomic concentration of $3 \times 10^{19} \text{cm}^{-3}$.

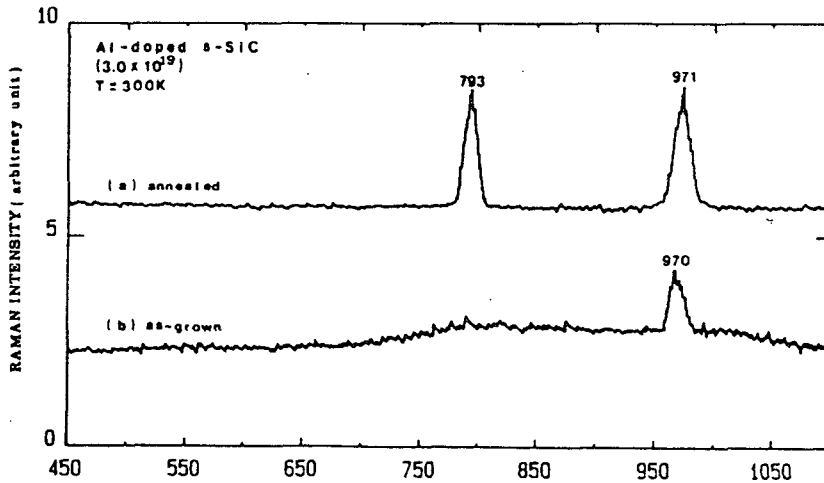


Figure 8. Room temperature Raman spectra for Al-doped ($3.0 \times 10^{19} \text{cm}^{-3}$) β -SiC; (a) annealed at 2073 °K for 300 s and (b) as-grown.

No additional peaks appear due to unactivated dopants or acceptors activated from Al dopants. The most striking difference in the spectra of the as-grown Al-doped sample with respect to the spectrum of the unannealed and annealed undoped β -SiC (Figure 7) is the appearance of a broad band in the range 750 to 1100 cm^{-1} . This band seems to replace the TO peak at 796 cm^{-1} which occurred for the as-grown undoped β -SiC sample. With respect to the LO peak for the undoped β -SiC, the intensity of the LO peak that appeared at 970 cm^{-1} in the analogous Al-doped film is reduced considerably, and the position is shifted to lower frequencies. The results indicate that the crystal structure of β -SiC thin film is not structurally perfect. The annealing process at 2073 °K for 300 s results in the broad band in the unannealed sample being replaced by a sharp TO peak at 793 cm^{-1} . The LO peak reappears at 971 cm^{-1} with greater intensity after annealing, but its position is still shifted to lower frequencies. After annealing, the intensity ratio of the LO to TO peaks is almost 1.

The spectrum of the N-doped SiC film ($7.4 \times 10^{19} \text{ cm}^{-3}$) shown in Figure 9.

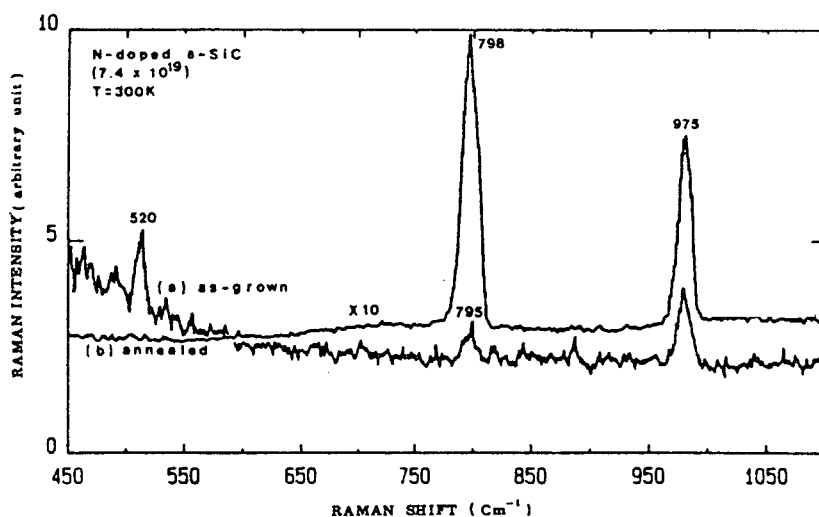


Figure 9. Room temperature Raman spectra for N-doped ($7.4 \times 10^{19} \text{ cm}^{-3}$) β -SiC; (a) as-grown and (b) annealed at 2073 °K for 300 s.

An interesting point in this spectrum is the appearance of the excess non-carbon bonded Si peak at 520 cm^{-1} . The appearance of this peak indicates that either N atoms replace C atoms or N atoms promote the formation of Si anti-site defects. These defects are produced by the occupation of C sites by Si. In both cases, several Si-Si like bonds are produced. The low frequency tail and the low intensities of the LO and TO peaks in the as-grown sample indicate

that introduction of N produces defects and disorder which are decreased during annealing. As indicated, the spectrum of the annealed sample shows sharp and intense peaks for both the LO and TO peaks. The non-carbon bonded Si-Si peak at 520 cm^{-1} also disappears in the annealed sample. From the disappearance of this latter peak one may tentatively conclude that N dopants promote the anti-site defects. This may be reasoned that if N dopants replace C atoms in SiC during growth, they would most likely remain in the C site after annealing and thus would not eliminate the non-carbon bonded Si peak. The intensity ratio of TO to LO peaks is 1.4 after annealing, since the intensity of the TO peak drastically increases. This value is significant, since the intensity of LO is usually greater than that of TO.

In the case of P doping ($1.2 \times 10^{17}\text{ cm}^{-3}$) in SiC, the spectrum in Figure 10 is very similar to that of the N-doped sample with respect to the appearance of the non-carbon bonded Si peak at 520 cm^{-1} .

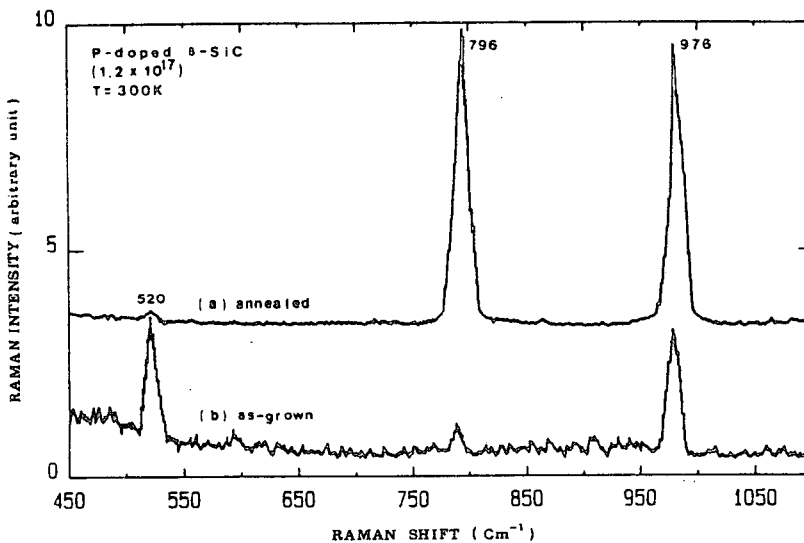


Figure 10. Room temperature Raman spectra for P-doped ($1.2 \times 10^{17}\text{ cm}^{-3}$) β -SiC; (a) annealed at $2073\text{ }^\circ\text{K}$ for 300 a and (b) as-grown.

This spectrum also shows low intensity LO and TO peaks and a low frequency tail. After annealing, the intensities of the LO and TO peaks increase considerably and a trace of the Si peak can still be observed. The intensity ratio of TO to LO is about 1.1.

The non-carbon bonded Si peak at 520 cm^{-1} is also observed in the spectrum of the unannealed B-doped SiC sample ($1.6 \times 10^{17}\text{ cm}^{-3}$), as shown in Figure. 11.

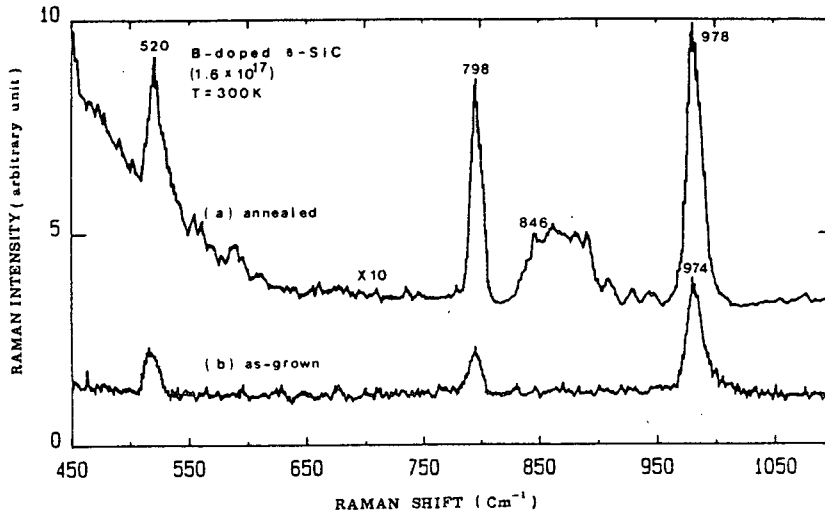


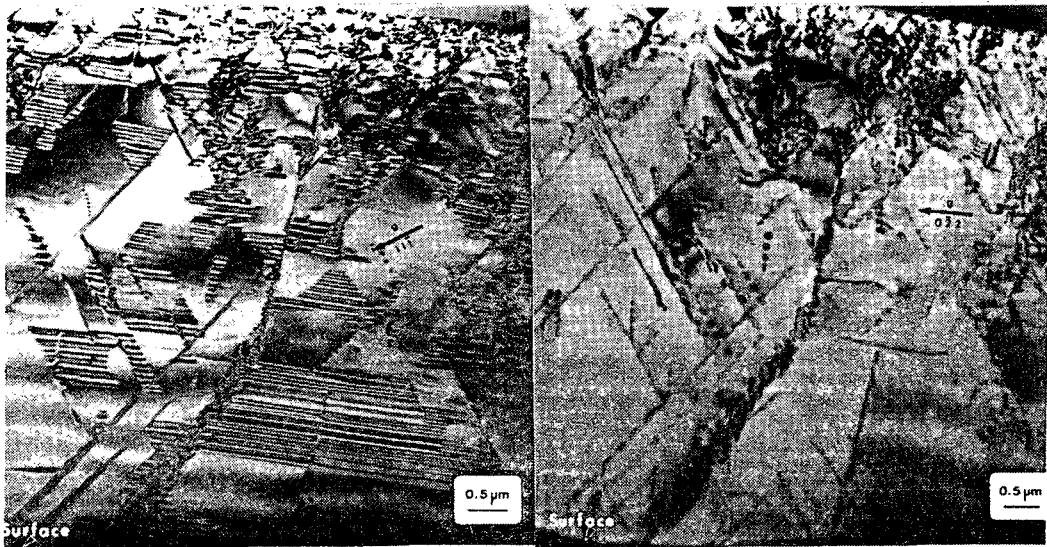
Figure 11. Room temperature Raman spectra for B-doped ($1.6 \times 10^{17} \text{ cm}^{-3}$) β -SiC; (a) annealed at 2073 °K for 300 s and (b) as-grown.

After annealing, a low frequency tail and several unidentified peaks appeared, and an increase in the intensity of the Si peak occurred. These changes indicate that B reacts with C and forms a second phase during annealing at 2073 °K for 300 s. The sample was examined by TEM in an attempt to visually observe this second phase; however, the results and discussion will be presented in the next section.

The effect of dopants on the Raman spectra of β -SiC is difficult to explain by the coupled LO-phonon-electron mechanism¹². Although an increase in the number of charge carriers occurs after annealing, the increase in the intensities of the LO and TO peaks occurs. This indicates that this mechanism should be ruled out as a possible explanation. Another possible explanation is that the added impurities may change the polarization properties of the allowed phonon modes or may result in the amorphization of the crystalline structure thereby circumventing the crystal-momentum selection rules. Even when the added impurities are not sufficient to alter the symmetry-based selection rules, the effect of the damage can manifest itself by broadening the allowed phonon modes and by shifting the observed mode frequencies.¹² These effects are the result of local stresses and strains arising from the difference in size between impurities and the sites in which they sit. These results are quite consistent with those obtained by IR spectra.

C. Cross-sectional TEM (XTEM)

The XTEM micrograph in Figure 12(a) and (b) reveals stacking faults with $g=11\bar{1}$ and dislocations with $g=02\bar{2}$, respectively, in the same area of an undoped β -SiC sample with a thickness of $15\ \mu\text{m}$.



(a)

(b)

Figure 12. XTEM micrographs showing the Si-SiC interface. (a) shows the presence of stacking faults with $g = 11\bar{1}$ (b) reveals the presence of dislocations with $g = 02\bar{2}$

These defects originate as a result of the mismatch in both lattice parameters and coefficients of thermal expansion. These mismatches also result in some residual elastic strain near the interface, as evidenced by the strain contrast. The stacking faults make 45° with or parallel to the interface, since, as noted above, these growth faults lie on (111) planes and the as-grown film on the interface is of (100) orientation.²¹

The XTEM micrographs of the doped β -SiC samples except the annealed B-doped sample are the same density and distribution of stacking faults and dislocations as that of the undoped sample and thus are not shown here. A microstructural anomaly in the form of a wide twin band near the Si/SiC interface was observed via XTEM in the annealed B-doped β -SiC film as shown in Figure 13.

The associated SAD patterns for the three different regions is also presented in this figure. The combined pattern in region b consists of the two diffraction patterns derived from regions a and c. This former pattern provides the evidence for twinning. This result is consistent with the results of IR absorption and Raman scattering. Thus the presence of B may induce twinning during annealing at 2073 °K; however, additional research must be conducted to clarify this point.

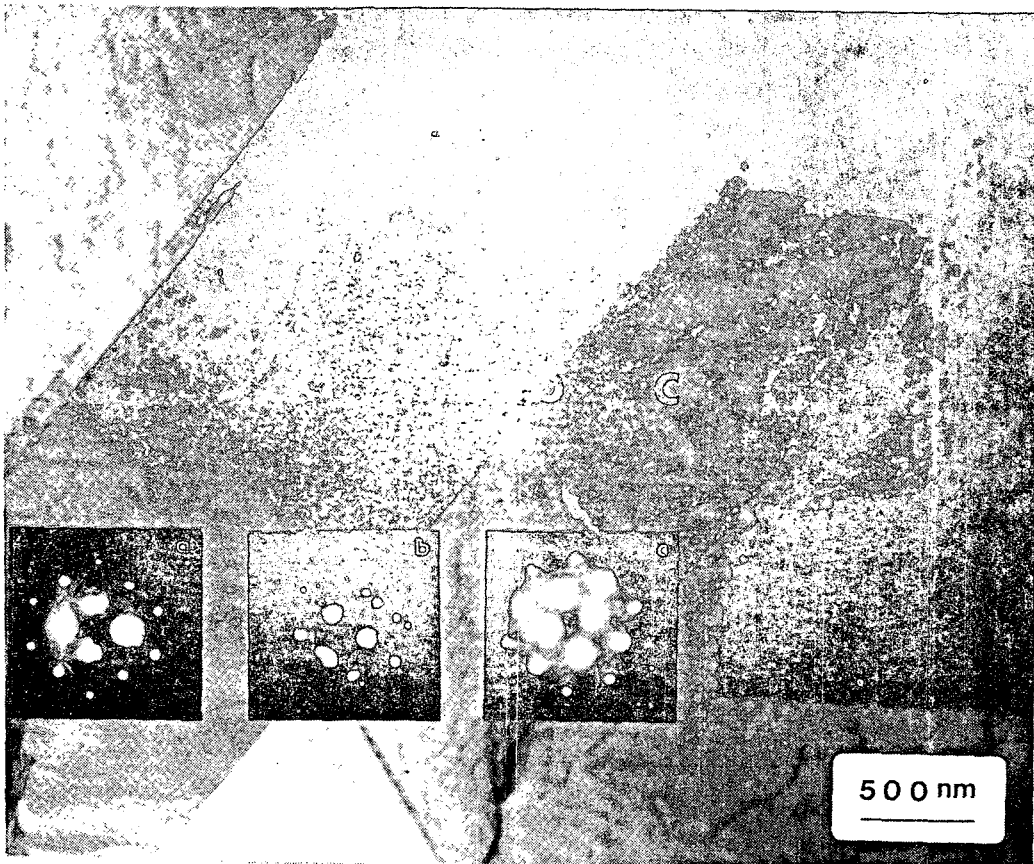


Figure 13. XTEM micrograph of an annealed (2073 °K, 300 s) heavily B-doped ($4 \times 10^{21} \text{ cm}^{-3}$) β -SiC film.

IV. Conclusions

The undoped and doped β -SiC thin films were characterized by IR and Raman spectroscopies. The IR absorption bands in the 400 to 1800 cm^{-1} region of IR transmission spectrum of β -SiC were assigned by the combinations of four phonon modes, of which frequencies were 373, 654, 768 and 855 cm^{-1} for TA, LA, TO and LO, respectively. It was found that the shape and positions of IR absorption bands were changed with the concentration and kind of dopants, that is, the broad and weak bands replaced the sharp and strong bands. At the same order of dopant concentration the IR absorption spectrum of β -SiC thin film was more affected by N dopant than by Al dopant. The IR absorption spectra of the lightly doped (B- and P-doped) β -SiC were less deformed than those of the heavily doped (Al- and N-doped) β -SiC.

After annealing at 2073 °K for 300 s, the IR absorption spectra of the heavily doped β -SiC became more similar to that of the undoped β -SiC. But the IR absorption spectrum of the B-doped sample annealed at 2073 °K for 300 s showed weak absorption bands and broad Reststrahlen bands.

Raman spectra of the 450 to 1100 cm^{-1} region for the doped β -SiC films showed the shift and broadening of two prominent first order Raman peaks, TO and LO, which were observed at 797 and 975 cm^{-1} , respectively, in Raman spectrum of the undoped β -SiC. Except Al-doped sample, Raman spectra of other doped samples also showed an additional peak, which represented the excess non-carbon bonded Si at 520 cm^{-1} .

Annealing of the doped β -SiC at 2073 °K for 300 s increased the intensity of Raman peaks drastically, shifted the position of Raman peaks to higher frequencies and cancelled the non-carbon bonded Si peak in Raman spectra. But the Raman spectra of the annealed B-doped β -SiC showed a low frequency tail and several unidentified peaks. XTEM micrographs of the annealed B-doped β -SiC revealed that twinning occurred during annealing. This result provides the explanation of the anomaly of IR and Raman spectra of the annealed B-doped β -SiC.

References

1. E. O. Johnson RCA Review 26, 163 (1965).
2. R. W. Keyes, Proc. IEEE 60, 225 (1972).
3. H. J. Kim and R. F. Davis, J. Appl. Phys. 60, 2897 (1986).
4. W. G. Spitzer, D. Kleinman and D. Walsh, Phys. Rev. 113, 133 (1959).
5. I. P. Akimchenko, L. M. Ivanova, A. A. Pletyrushkin and G. K. Rasulova, Inorg. Mat. 14, 523 (1978).
6. W. G. Spitzer, D. Kleinman and D. Walsh, Phys. Rev. 113, 127 (1959).
7. H. G. Lipson, in Silicon Carbide, A High Temperature Semiconductor, Eds. J. R. O'Connor and J. Smiltens, Pergamon Press, New York (1960), p371.
8. L. Patrick and W. J. Choyke, Phys. Rev. 123, 813 (1961).
9. R. B. Campbell, IEEE Trans. Indus. Electron. IE-29, 124 (1982).
10. S. S. Mitra, O. Brafman, W. B. Daniels and R. K. Crawford, Phys. Rev., 186, 942 (1969).
11. D. W. Felden, J. H. Parker, Jr., W. B. Daniels and R. K. Crawford, Phys. Rev. 173, 787 (1986).
12. R. B. Wright and D. M. Gruen, Rad. Eff., 53, 133 (1977).
13. D. Olego and M. Cardona, Phys. Rev. B. 25, 1151 (1982).
14. P. J. Colwell and M. V. Klein, Phys. Rev. B, 6, 498 (1972).
15. M. Chandrasekhar, M. Cardona and E. O. Kane, Phys. Rev. B, 16, 3579 (1977).
16. H. Engstrom and J. B. Bates, J. Appl. Phys. 50, 2921 (1979).
17. D. T. Hon, W. L. Faust, W. G. Spitzer and P. F. Williams, Phys. Rev. Lett. 25, 1184 (1970).
18. G. Irmer, V. V. Toporov, B. H. Bairamov and J. Monecke, Phys. State. Sol. (b) 119, 595 (1982).
19. S. Venugopalan, A. Petrou, R. R. Galazka and A. K. Ramdas, Phys. Rev. B, 25, 2681 (1982).
20. W. L. Choyke, D. R. Hamilton and L. Patrick, Phys. Rev. 133, A 1163 (1964).
21. H. J. Kim and R. F. Davis, J. Electrochem. Soc. 133, 2350 (1986).
22. C. H. Carter, Jr., J. A. Edmond, J. W. Palmour, J. Ryu, H. J. Kim and R. F. Davis, to be published in MRS Symposia Proceedings on Microscopic Identification of Electronic Defects in Semiconductors, San Francisco, CA, 1985.

全體討論(薄膜技術)

座長 李 銓

야마기시씨에게 질문 : (조상희)

〈問〉; 내마모성 재료 개발에서 ion plating process 로 coating 하는 경향인데, 전자세라믹스와 전기적 성질의 개발에 이 process 가 어떻게 이용되고 있는지 ?

〈問〉; 일본에서 지금 ion plating 장치는 어떻게 개발되고 있으며 또 어떤 방향으로 이용되고 있는지 ?

말해 주십시오.

〈答〉; 어려운 질문이며, 한마디로 답변하기 어렵다.

〈問〉에 대하여 ;

내마모성 재료 이외의 분야에의 응용도 ion process 가 충분히 가능하리라고 생각 합니다. 그러나 ion plating 이 최상의 방법인지의 여부에 대하여는 잘 모르겠습니다. 경우에 따라서는 sputtering, 진공증착, 이온주입 등의 기타 process 도 이용할 수 있으며 그런 광범위내에서 선택할 수 있는 문제이며 반드시 이용되는 분야가 있으리라 생각합니다.

유감이지만 나는 어디까지나 내마모성 재료의 추구에 전념하였을 뿐 이므로 자기 연구 영역 이외에 대하여 말할 역량이 없습니다.

〈問〉에 대하여 ;

일본에서의 연구방향의 하나는 막의 품질을 어떻게 향상시키느냐 하는 것에 있습니다. 즉 TiN을 ion plating process 를 이용하여 coating 할 경우 그 막의 물성이 틀리게 나타나는데 이것은 같은 TiN을 coating 했다고 생각해도 coating 조건에 따라 막재질에 여러 성질의 차가 나타나기 때문입니다. 이를 역으로 말하면 같은 TiN을 coating 해도 생각에 따라 조건을 달리했을 경우 얻어진 막의 물성에는 중국의 국한치가 있다는 것을 시사하는 것입니다. 그래서 막재질을 점점 좋게 한다는 것 즉 예로서 내마모성에 적합한 막재질의 물성을 어디까지 향상시킬 수 있느냐 하는 것은 장치의 plasma 의 파라메타를 여러가지로 조절함으로써 막재질의 품질향상이 추구되어 가며 우리 뿐 아니라 일본 각처에서 여러가지 process 로 열심히 어프로치하고 있는 실정입니다.

또 하나는 막재질이 언제까지나 TiC, TiN에 국한하지 않고 더욱 보다 좋은 막재질, 보다 좋은 내마모성이 발휘되는 막재질을 적어도 우리는 개발하고 있으며, 다른 경쟁자들도 꼭

하고 있으리라 생각합니다.

예로서 최종적으로는 경도만을 택한다면 장래상으로는 CBN의 coating 일 것이며 다이아몬드의 coating 일 것이며 우리는 이런 방향도 내마모성 분야의 막재질로서 관과할 수 없으며 연구를 계속하고 있는 실정입니다. 세다까 선생의 연구를 충분히 참고 하시기 바라며 내마모성을 주제로 하고있는 여러가지 연구개발은 반드시 같은 경향이 아닌가 하고 생각합니다.

쓰까모도씨에게 질문 ; (김병호)

<問>; Substrate에 Al₂O₃을 coating 할 때에 substrate와의 사이에 ε - phase의 interface가 생기며 그래서 Al₂O₃의 직접 coating이 어려우며 물성이 나쁩니다. Coating막의 물성이 brittle해지는 mechanism은 무엇이며 substrate에 Al₂O₃를 coating하기 전에 특별한 coating층을 형성시킨 연후에 Al₂O₃를 coating하면 양질의 두꺼운 Al₂O₃ coating 막을 얻는다 했는데 그것에 대하여 말씀해 주십시오.

<答>; Substrate에 Al₂O₃를 coating할 때 그 층을 두껍게 하면 substrate 쪽에 최초로 Al₂O₃의 ε - phase가 생성됩니다. 그런 경우 강도가 약화됩니다. 보통 substrate 위에 Al₂O₃를 직접 coating 한다는 것은 어려운데 왜 그런가하면 산화물인 Al₂O₃로 인하여 substrate 쪽이 산화되고 그래서 밀착성이 불량해지는 것입니다. 그래서 TiC, TiN, 등의 층을 inter layer로서 substrate 위에 미리 형성시킨 뒤 Al₂O₃ coating을 시행하며 이때 Al₂O₃로 인한 내마모성을 더욱더 향상시키고 싶다면지 절삭속도를 더욱더 증가시키고 싶을 때 Al₂O₃층은 두껍게 하는것이 좋습니다. 그런데 Al₂O₃층을 두껍게 coating할 경우 보통의 방법으로는 결정립이 크게 되는데 이것을 억제하기 위하여는 하나의 방법으로서 CVD의 경우에는 온도가 높아서 모재로부터의 확산이 일어나고 또한 입자 자체의 성장이 빠릅니다. 그러므로 중간층으로서 특별한 층을 형성시키고 그럼으로써 핵의 생성을 증가시키고 결정성장을 억제하고 그래서 결정입자의 크기를 작게해야 합니다.

그런데 단순히 특수물질층을 형성시키는 것 만으로는 아니되고 coating의 여러조건을 조절하지 않으면 아니된다는 것을 알아야 합니다.

김형준박사에게 질문 : (이전)

<問>;김박사는 오늘 세다까선생에게 많은 질문을 하는 것을 보았습니다. 그런데 아시다시피 세다까박사는 다이아몬드박막합성에 10년이란 장구한 세월에 걸친 끈질긴 연구를 계속한 결과 세계 최초로 다이아몬드박막을 합성하는데 성공한 분입니다.

그런 점에서 김박사의 현 연구영역으로 보나 교육적 배경으로 보나 앞으로 다이아몬드박막 합성에 관심을 갖고 연구를 했으면 하는데 어떻습니까?

연구에 대한 제반여건이 대단히 어려우나 내 생각으로는 우리나라에서도 누군가가 장래를 위하여 다이아몬드박막의 합성에 연구를 착수하여야 한다고 생각합니다.

<答>; 그래서 제가 관심이 많아서 질문을 많이 했습니다. 아까 세다까선생에게 Si-substrate 와 다이아몬드박막 사이에 SiC가 생기지 않았느냐고 질문했더니 생긴다고 답변했습니다. 그것은 SiC의 converted layer가 생겼다는 말입니다. 저도 지금과 같은 경우를 실험해 보았는데, 일단 silicon-source 가스를 넣지않고 carbon-source 가스로서 에틸렌으로 계속 deposition을 시켜 보았을 때 substrate 위에 흑색의 입자가 많이 생겼었습니다. 이 표면조직을 scanning analytical microscope로 관찰했을 때 그것이 SiC의 입자일 것이라고 간주했었는데 오늘 세다까선생의 답변을 듣고 보니 그것이 다이아몬드입자가 아니었나 하는 생각이 듭니다.

제가 관심이 많기 때문에 오늘 세다까선생께 이런 점들에 관하여 많은 것을 질문했는데 여건이 허락되면 저도 다이아몬드박막을 합성해 보고 싶습니다.

座長:

한 우물을 파고 또한 깊이 파라는 격언이 있는데 오늘 여기 이 자리에 열의에 가득찬 많은 젊은 과학도, 공학도, 연구원, 기술자들을 위하여 그 교훈이 심각히 받아들여 졌으면 하는 바람에서 김박사에게 질문을 했던 것입니다.

세다까선생님! 당신은 한 좁은 연구분야에서 장구한 세월동안 침식을 잊고 연구한 보람이 있어 세계 최초로 다이아몬드박막을 합성하는 연구 개발에 성공한 분으로 알고 있습니다. 앞서 많은 질문을 한 젊은 학자를 포함하여 이 방면의 연구에 관심이 있는 한국의 많은 학자와 학문적인 교류가 이루어졌으면 다행으로 생각하겠습니다.

座長:

오늘 활발한 질의 및 답변을 보면서 앞으로 우리는 이런 기회를 더 많이 가졌으면 하는 공감을 가졌으리라 믿습니다. 이것으로 종합토론을 맺겠습니다.

감사합니다. 끝.